Journal of Structural Geology, Vol. 15, No. 1, pp. 69 to 78, 1993
Printed in Great Britain

0191-8141/93 $06.00+0.00

A new method for the geometrical classification of large data sets of folds

FERNANDO BASTIDA

Departamento de Geología, Universidad de Oviedo, 33005 Oviedo, Spain

(*Received* 17 *March* 1992; *accepted in revised form* 4 *July* 1992)

Abstract—The classification proposed here for folded layers is based on the use of two parameters, p_1 and p_2 (modified to p_1' and p_2') which are related to the variation in slope of the curves that describe orthogonal thickness vs dip. Each fold limb is represented by a point on a p_1'–p_2' diagram. From p_1' and p_2' it is possible to obtain a one-dimensional statistical variable (intercept value t_{90}') which characterizes the geometry of folds and complements the proposed classification. The fold classification method suggested is easy to use and it has considerable advantages in the geometrical analysis of large sets of folds. In addition, it can be applied to the theoretical analysis of fold geometry, to the comparative regional studies of fold and to the analysis of geometrical variations in a folded multilayer.

INTRODUCTION

THE knowledge of fold geometry is a basic requirement to investigate folding mechanisms. Owing to the abundance of this type of structure in nature, it is necessary to have classifications which allow information about fold geometry to be organized and statistically analysed. Such working tools must allow the comparative study of large groups of folds. The morphological description of folds has focused on two aspects: the geometry of single folded surfaces and the geometry of folded layers.

The fold classification proposed by Hudleston (1973a) for the profiles of cylindrically folded surfaces was a significant advance, because the geometry of each profile is characterized as a two-dimensional statistical variable. An alternative classification has been proposed by Twiss (1988); however, its application to natural folds has not yet been widely used.

Based on a study of thickness variations in a folded layer, Ramsay (1962) suggested that similar and parallel folds represent the two end members of a range of possible fold geometries. Subsequently, Ramsay (1967, pp. 359–369) developed a fold classification which was based on the dip-isogon pattern and variations with the dip (α) of the thickness perpendicular to layering (t_α') or parallel to axial surfaces (T_α') (Fig. 1a). In this model, each limb is characterized by a t_α', curve whose position and geometry determine the class of fold. Ramsay differentiated three fold classes: class 1, class 2 (similar folds) and class 3, with three subclasses of class 1 folds: 1A, 1B (parallel folds) and 1C. The geometry of these classes is shown in Fig. 1(b). In order to make the classification more precise, Ramsay (1967, p. 370) also suggested using the first two derivatives of the thickness in comparison to the dip, since the fold class is controlled by the slope variation of the tangent to the curve t_α', rather than by its position inside the fields in Fig. 1(b).

A problem with Ramsay's classification is the difficulty in obtaining the best location of the reference thickness (t_0) to determine t_α'. In order to solve this problem, Hudleston (1973a) modified Ramsay's classification by the application of a new parameter (Φ_α), defined as the angle between the normal to the tangents drawn to either fold surface at angle of dip α, and the

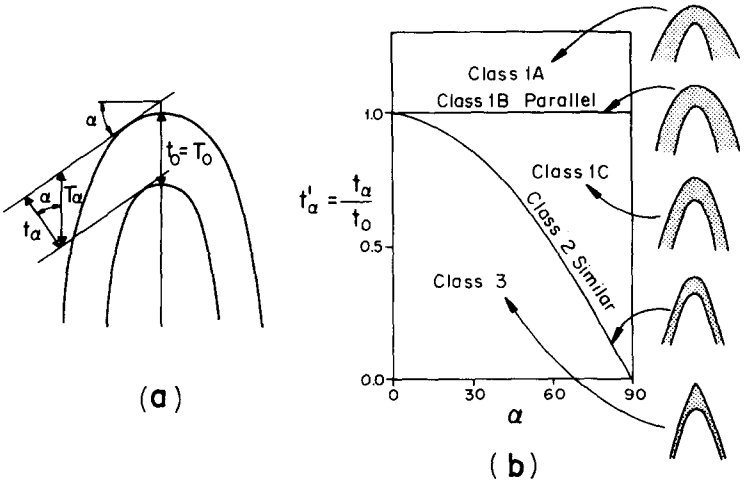

Fig. 1. (a) Definitions of orthogonal thickness (t_α) and thickness parallel to axial surface (T_α) of a folded layer (after Ramsay 1967, p. 361). (b) Fold types defined on the t_α'–α diagram (after Ramsay & Huber 1987, p. 349).

isogon. However, Ramsay's classification has been the most commonly used until the present.

Subsequently, Treagus (1982) proposed a fold classification that relates the geometry of a fold to the cleavage. This classification is based on the variation between the cleavage trace and the normal to bedding, defined as the β angle. This classification does not replace that of Ramsay or Hudleston, but represents a complement to them.

Ramsay's classification provides an excellent tool for analysing the geometry of single folds. However, its application to natural folds presents some difficulties. First, unless done by computer, the analysis is very laborious. Second, it is unsuitable for statistical analysis of large data sets. Yet, such sets are frequent, whether in outcrops of a region or in individual multilayers. In such cases, comparing large numbers of t'_α curves is difficult, because it must be done visually. One example of such difficulties can be seen in Davis's work (1975, fig. 5) on the folding off a gneiss dome complex in the Rincon Mountains (Arizona); the t'_α curve swarms which appear in the diagrams of the different domains considered make it hard to draw conclusions about the geometry of the folded layer sets, based on a truly quantitative analysis.

The need to synthesize the results obtained from Ramsay's classification was considered by Hudleston (1973b), who analysed a large number of minor folds developed in the Moine rocks of Monar (Scotland). In order to transform a t'_α curve into a single parameter, Hudleston projected t'^2_α against $\cos^2 \alpha$ and obtained the intercept value of the best-fit straight line. Although this method is useful, it is very laborious, because it requires each fold to be classified by Ramsay's method and the curve of each limb to be fitted by means of a least-squares linear regression program. Besides, the method implies a loss of information on individual fold geometry. Hudleston (1973b) complemented it by the use of t'_α curves.

The aim of this paper is to establish a simple classification of folded layers, based on Ramsay's classification, but which is quicker to use than the preceding classifications, and which allows the representation of fold limb shape as a single point on a diagram. From this classification, it is very easy to obtain an intercept value, comparable to the one used by Hudleston (1973b), which allows the geometry of folded layers to be analysed by means of a one-dimensional statistical variable. This method will greatly facilitate statistical analysis of large data sets of folded layers.

BASIS OF THE FOLD CLASSIFICATION METHOD

Begin with a t'_α curve from a fold limb, in which point O represents the hinge (Fig. 2). The curve must be continuous; experience shows that most curves have a simple geometry, with an extreme value of t'_α, often the maximum, at the origin, and with the other extreme

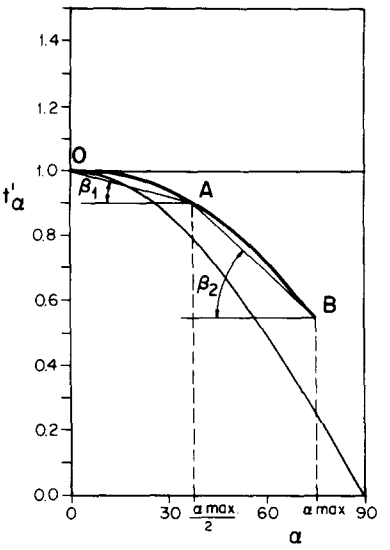

Fig. 2. Definition of angles β_1 and β_2 from the t'_α curve.

value at the other end of the curve. Two parameters that allow the best possible description of the geometry of the curve must be found. In Fig. 2, it is required that the abscissa scale for 90° equals 0.9 on the ordinate scale (t'_α). Consider two points, A and B. A is the point of the curve where the abscissa equals $\alpha_{max}/2$, and B the final point of the curve with an abscissa α_{max}. Draw the line segments, OA and AB, and define two parameters, p_1 and p_2, as:

$$p_1 = \tan \beta_1 = \frac{100(1 - t'_{\alpha_{max}/2})}{\alpha_{max}/2}$$
$$p_2 = \tan \beta_2 = \frac{100(t'_{\alpha_{max}/2} - t'_{\alpha_{max}})}{\alpha_{max}/2}. \quad (1)$$

These parameters can be used to describe the geometry of the t'_α curve. Parameters p_1 and p_2 represent mean slopes of parts of the curve (note that these parameters are not the same as P_1 and P_2 in Ramsay 1967, pp. 350–351). Thus a simple p_1 vs p_2 graph (Fig. 3) offers a means of classifying folds as each fold limb can be represented by a single point. The line corresponding to the parallel fold (Ramsay's subclass 1B) in Fig. 1(b) will lie at the origin on the p_1–p_2 diagram in Fig. 3. For $\alpha_{max} = 90°$, the curve corresponding to similar folds (Ramsay's class 2) in Fig. 1(b) will be represented by point 2 in Fig. 3. The graph (Fig. 3) contains several fields and lines on which points that represent fold classes are plotted. The 1A, 1C and 3 fold classes of Ramsay's classification lie on three of these fields. The other fields and all of the lines represent folds composed of two different classes in Ramsay's classification, one class corresponding to parameter p_1, and the other to p_2. For instance, field 3–1C will represent folds that are of Ramsay's class 3 for $\alpha < \alpha_{max}/2$ and of class 1C for $\alpha > \alpha_{max}/2$.

Figure 4 shows representative t'_α curves for the different fields of the p_1–p_2 diagram. As the diagram shows, the fold class is determined by the slope of the curve t'_α and not strictly by the field in the α–t'_α diagram in which

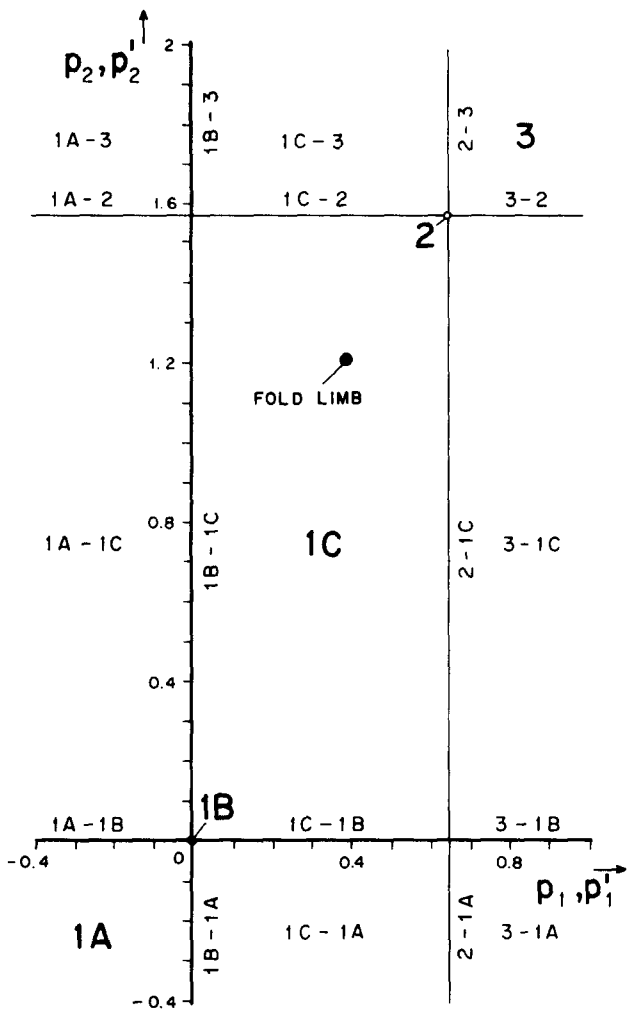

Fig. 3. Fields and lines defined on the p_1–p_2 graph, and the modified graph (p'_1–p'_2), and their corresponding fold classes.

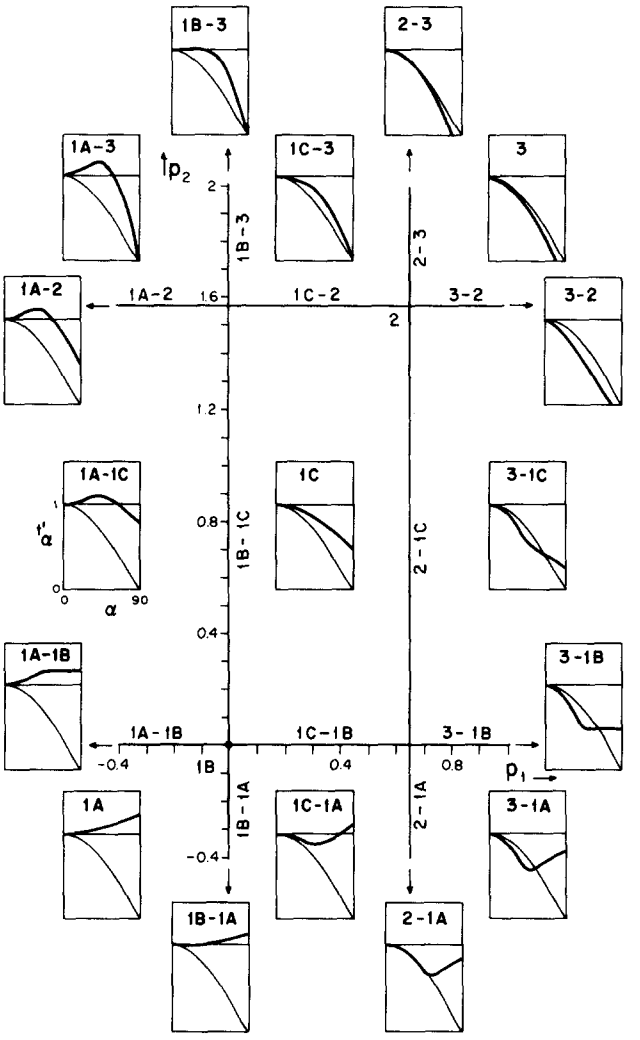

Fig. 4. t'_α curves representative of the folds corresponding to different fields and lines of the p_1–p_2 diagram.

the curves are situated. In this sense, the p_1–p_2 diagram sometimes represents the fold class better than the curve t'_α itself, since p_1 and p_2 closely define the mean curve slope.

Since natural folds are not generally isoclinal, α_{max} will not usually be 90°. Some problems derive from this fact; for example, the limb shown in curve OAB in Fig. 5(a) will be represented on the p_1–p_2 diagram (Fig. 5b) by a point S (s_1, s_2) situated within the field corresponding to class 1C folds and will not plot at the same position as one representing the similar fold limb given by OAB' (point S'(s'_1, s'_2) in Fig. 5b). This means that folds which belong to a given class in the t'_α–α diagram lie within different fields on the p_1–p_2 diagram, depending on the maximum limb dip. This is clearly not acceptable. To avoid this, it is necessary to ensure that any t'_α curve corresponding to a similar fold shape, as is the case for OAB in Fig. 5(a), is represented by point S in Fig. 5(b), regardless of the value of α_{max}. To do this, the results are transformed so that the sides of parallelogram ORST become those of parallelogram OR'S'T'. This can be done by means of a transformation with matrix:

$$\mathbf{A} = \begin{pmatrix} s'_1/s_1 & 0 \\ 0 & s'_2/s_2 \end{pmatrix} = \begin{pmatrix} \dfrac{\alpha_{max}(2-\sqrt{2})}{180[1-\cos(\alpha_{max}/2)]} & 0 \\ 0 & \dfrac{\alpha_{max}\sqrt{2}}{180[\cos(\alpha_{max}/2)-\cos\alpha_{max}]} \end{pmatrix} \quad (2)$$

where the angles are expressed in degrees. The displacements of the sides of rectangle ORST derived from this transformation are indicated by the vectors represented in Fig. 5(b).

As the elements in the leading diagonal of **A** are functions of α_{max}, a fixed transformation can be deduced for each value of α_{max}. Consider now curve OCD (Fig. 5a) which has the same value of α_{max} as OAB. Point P will represent values p_1 and p_2 of curve OCD on the diagram of Fig. 5(b). This point undergoes the transformation defined by matrix **A**, and becomes point P'(p'_1,p'_2), whose co-ordinates, according to expressions (1), will be given by:

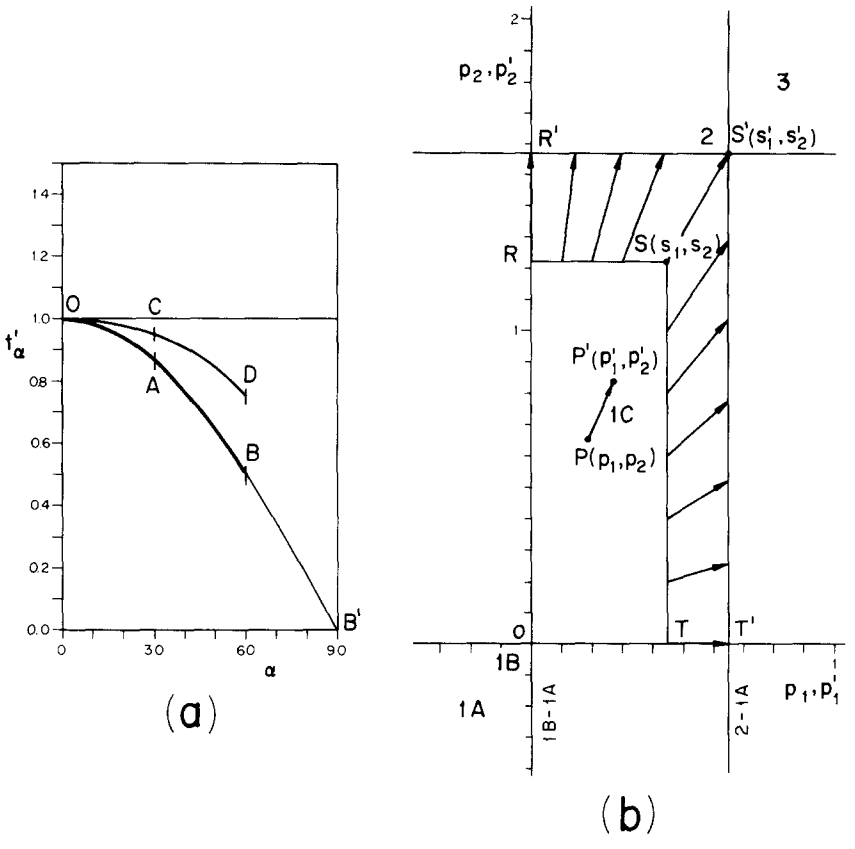

Fig. 5. Problem posed when $\alpha_{max} < 90°$ in a t'_α curve. (a) t'_α curves of a similar fold (OAB) and a 1C class fold (OCD) with $\alpha_{max} < 90°$. (b) Point S, representing curve OAB, does not match S', the point of the similar fold when $\alpha_{max} = 90°$. It also illustrates the displacement vectors involved in the transformation of rectangle ORST into OR'S'T'. S is transformed into S' and P, representing of the curve OCD, into P'.

$$p'_1 = (1 - t'_{\alpha_{max}/2})(2 - \sqrt{2})/0.9[1 - \cos(\alpha_{max}/2)] \quad (3)$$

$$p'_2 = (t'_{\alpha_{max}/2} - t'_{\alpha_{max}})\sqrt{2}/0.9[\cos(\alpha_{max}/2) - \cos\alpha_{max}]. \quad (4)$$

These are the values that are plotted on the modified p_1–p_2 diagram (p'_1–p'_2 diagram). Similarly, each t'_α curve with $\alpha_{max} < 90°$ will undergo the transformation defined in (2).

The t'_{90} value obtained from expressions (3) and (4), for $\alpha_{max} = 90°$, can be used as an intercept value comparable to that used by Hudleston (1973a). This value is given by:

$$t'_{90} = 1 - 0.45(p'_1 + p'_2) \quad (5)$$

from which the geometry of folded layers can be analysed as a one-dimensional statistical variable.

Geometrical properties of the ponts on the p'_1–p'_2 *diagram*

In order to know if the points on the p'_1–p'_2 diagram are a good representation of the geometry of folded layers, it is important to relate the geometry of a t'_α curve (OAB in Fig. 6a) to the position of the corresponding point on the p'_1–p'_2 diagram (R in Fig. 6c).

The t'_α curve may be divided into two sections: OA and AB (Fig. 6a). The first part is characterized by the parameter p'_1 and the second part by the parameter p'_2. From expressions (3) and (4), for $\alpha_{max} = 90°$, t'_{45} and t'_{90} can be found, whose values allow points A' and B' to be defined. The slopes (with reversed sign) of segments OA' and A'B' are equal to p'_1 and p'_2, respectively.

For the section characterized by p'_1, from points $A(\alpha_{max}/2, t_{\alpha_{max}/2})$, $A'(45, t'_{45})$ and R (p'_1,p'_2) it is easy to demonstrate that the following relations are satisfied (Figs. 6a & c):

$$a_1/a_2 = a'_1/a'_2 = a''_1/a''_2 \quad (6)$$

or in the same way,

$$\frac{1 - t'_{\alpha_{max}/2}}{t'_{\alpha_{max}/2} - \cos(\alpha_{max}/2)} = \frac{1 - t'_{45}}{t'_{45} - \sqrt{2}/2} = \frac{0.9\,p'_1}{2 - \sqrt{2} - 0.9\,p'_1}. \quad (7)$$

These expressions indicate that, for this section of the t'_α curve, the transformation preserves the distance ratio of points A, A' and R with regard to the lines representative of class 1B and 2 folds.

However, for the section characterized by p'_2, analogous relationships to those of (6) and (7) are not, in general, satisfied. This is due to the position of this section on the α–t'_α diagram, which is a factor of the location of point A (fold class is determined by the slope variation of the t'_α curve and not its position). This is the reason why Ramsay (1967, p. 370) used the derivative $(dt'_\alpha/d\alpha)$ to make his classification more accurate. Ordinate p'_2 of point R on the p'_1–p'_2 diagram is determined by the value of α_{max} and the second section mean slope of

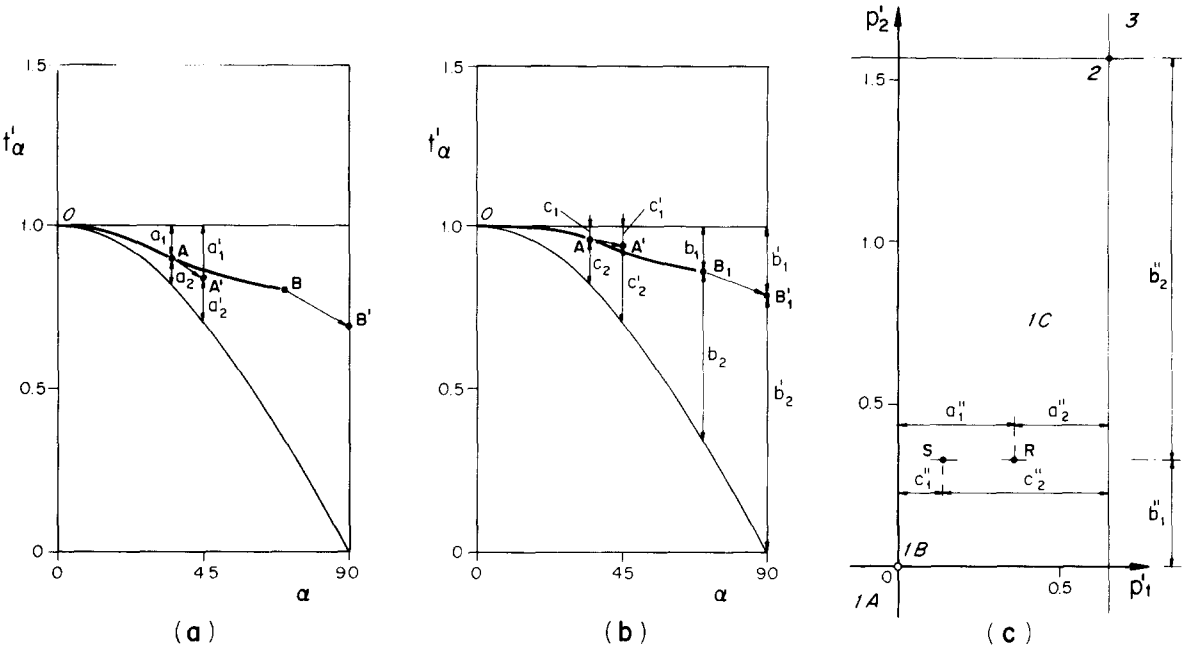

Fig. 6. (a) & (b) Distances that characterize the position of the points with abscissae α_{max} and $\alpha_{max}/2$ on t'_α curves, and their transformed points. (c) Distances which characterize the position of the points representative of t'_α curves of (a) and (b) on the p'_1–p'_2 diagram.

the t'_α curve, showing correctly the fold class for this section. The b''_1/b''_2 value on the p'_1–p'_2 diagram (Fig. 6c) is the same as b'_1/b'_2 value on the α–t'_α diagram (Fig. 6b), for a section A_1B_1 with the same slope and α_{max} as AB, if:

$$b_1/b_2 = b''_1/b''_2. \tag{8}$$

Furthermore, analogous relations to (6) and (7) are satisfied for the second section of the t'_α curve only if condition (8) is satisfied. In such a case (OA_1B_1 curve in Fig. 6b, and point S in Fig. 6c), the distance ratios for both sections become equal (Figs. 6b & c),

$$c_1/c_2 = c'_1/c'_2 = c''_1/c''_2 = b_1/b_2 = b'_1/b'_2 = b''_1/b''_2 = K \tag{9}$$

or in the same way,

$$\frac{1 - t'_{\alpha_{max}/2}}{t'_{\alpha_{max}/2} - \cos(\alpha_{max}/2)} = \frac{1 - t'_{45}}{t'_{45} - \sqrt{2}/2} = \frac{1 - t'_{\alpha_{max}}}{t'_{\alpha_{max}} - \cos\alpha_{max}} = \frac{1 - t'_{90}}{t'_{90}} = \frac{0.9\,p'_1}{2 - \sqrt{2} - 0.9\,p'_1} = \frac{0.9\,p'_2}{\sqrt{2} - 0.9\,p'_2} = K. \tag{10}$$

Expression (10) implies that

$$p'_2 = \frac{\sqrt{2}}{2 - \sqrt{2}}\,p'_1. \tag{11}$$

Substituting (11) in (4), equating expressions (3) and (4), and finding $t'_{\alpha_{max}}$, then,

$$t'_{\alpha_{max}} = t'_{\alpha_{max}/2} - \frac{(1 - t'_{\alpha_{max}/2})[\cos(\alpha_{max}/2) - \cos\alpha_{max}]}{1 - \cos(\alpha_{max}/2)} \tag{12}$$

which is the other condition implied by equalities (10).

A set of t'_α curves which satisfy the conditions expressed by (10), for different values of K, are shown in Fig. 7(a). Every section in a given curve which starts from point O(0,1) will be represented by the same point on the p'_1–p'_2 diagram. The points of the p'_1–p'_2 diagram which represents the curves of Fig. 7(a) are shown in Fig. 7(c). These points are situated along diagonal OT, so that relation r/s is equal to the corresponding value of K. This accounts for the fact that the condition expressed by (11) is the equation of the diagonal.

Figure 7(b) represents a set of t'_α curves which do not satisfy the conditions expressed by (10). Every curve on this figure corresponds to the same point on the p'_1–p'_2 diagram (point D in Fig. 7c). An overestimation of the curve section that has the highest slope would result from an extrapolation of these curves. However, the curve sections which correspond to p'_1 and p'_2 are weighted by the transformation defined in (2).

APPLICATION OF THE FOLD CLASSIFICATION METHOD

To classify a fold using the p'_1–p'_2 method the procedure is as follows.

(1) Thicknesses t_0, $t_{\alpha_{max}}$ and $t_{\alpha_{max}/2}$ and the angle α_{max} are measured and then $t'_{\alpha_{max}} = t_{\alpha_{max}}/t_0$ and $t'_{\alpha_{max}/2} = t_{\alpha_{max}/2}/t_0$ are determined.

(2) Expressions (3) and (4) or the graphs of Fig. 8 are used to determine p'_1 and p'_2 and then these parameters are represented on the diagram. In order not to lose the α_{max} value with the classification, different symbols can be used for the points on the diagram representing the different intervals of the α_{max} values.

Expression (5) can be used to obtain the intercept value t'_{90}.

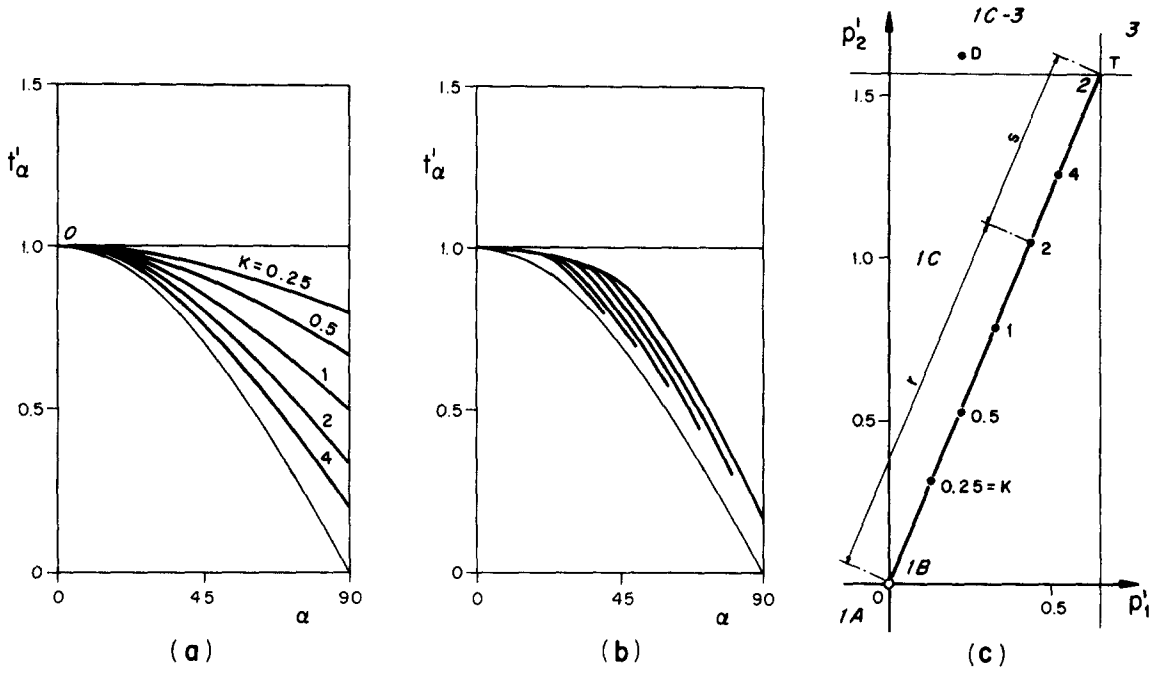

Fig. 7. (a) Set of t'_α curves which satisfy expression (9). (b) Set of t'_α curves which do not satisfy expression (9) (see text for explanation). (c) Points representative of t'_α curves of (a) and (b) on the p'_1–p'_2 diagram.

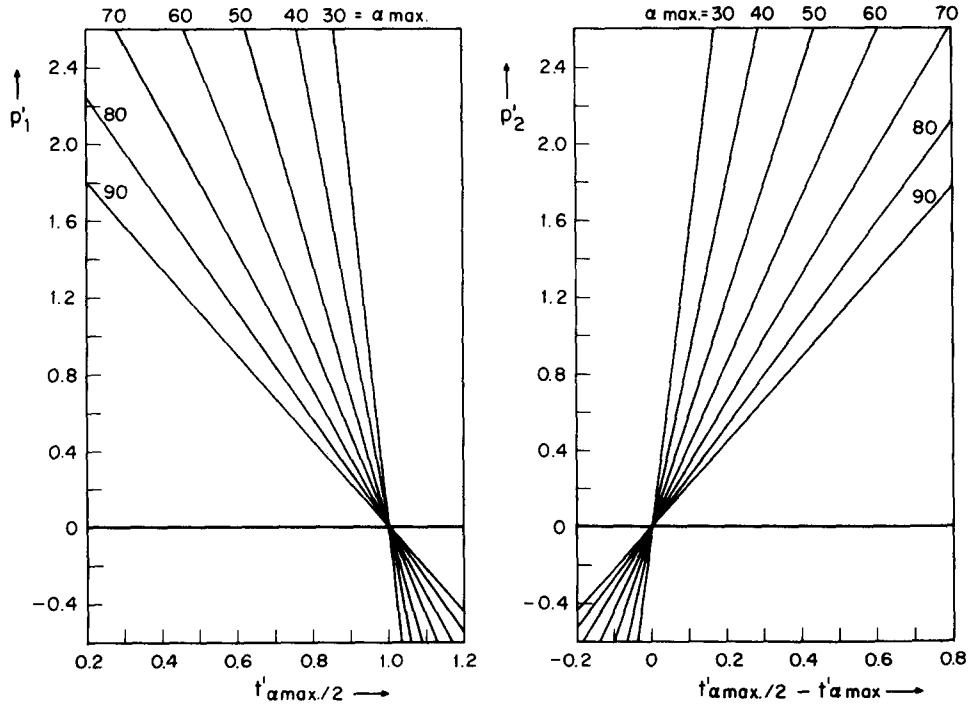

Fig. 8. Graphs to obtain p'_1 and p'_2 values from $t'_{\alpha_{max}}$ and $t'_{\alpha_{max}/2}$.

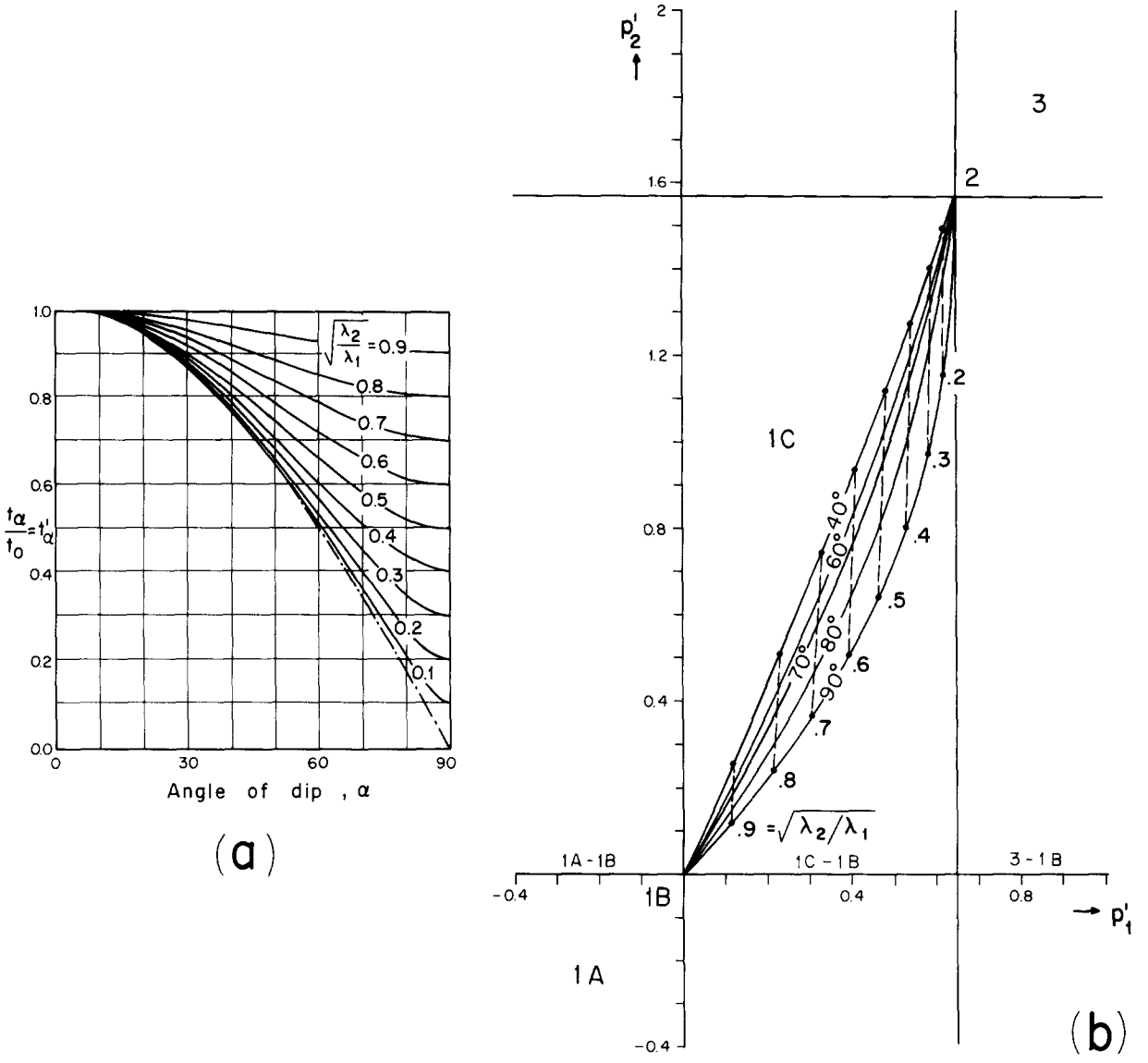

Fig. 9. (a) t'_α curves of flattened parallel folds (after Ramsay 1962, 1967, p. 413). (b) Paths defined by flattened parallel folds on the p'_1–p'_2 diagram for different values of α_{max} (situated on the curves); the dotted lines link points with equal flattening values.

Examples

In order to demonstrate the applicability of the classification method, three different cases have been considered.

(1) *Flattened parallel folds*. The method of the p'_1–p'_2 diagram has been applied to the t'_α curves deduced by Ramsay (1962, 1967) for flattened parallel folds (Fig. 9a). Figure 9(b) shows that the points representing these curves on the p'_1–p'_2 diagram define a trajectory within field 1C for each α_{max} value. As the amount of flattening increases, the point shifts from the origin (parallel folds) to the point representing similar folds. For any given flattening ($\sqrt{\lambda_2/\lambda_1}$), as α_{max} increases, the points of Fig. 9(b) come closer to the line 1C–1B. This is due to the fact that, for high dips, the t'_α curve slope decreases and the fold approaches class 1B, which is recorded on the p'_1–p'_2 diagram by a reduction of the p'_2 value.

(2) *Folds in the West Asturian-leonese Zone (Variscan belt, NW Spain)*. Mesoscopic folds in the same generation (F_1), deforming lower Palaeozoic quartzitic rocks from two different units of this zone (Navia and Mondoñedo Nappe units) (Bastida 1980) have been classified (Fig. 10). Navia Unit rocks show lower deformation and metamorphic grade than those in the Mondoñedo Nappe Unit and foliation (S_1) is present in both units. The plots of the Mondoñedo Nappe folds (p'_1–p'_2 diagram and intercept values histogram) show the centre of gravity location in p'_1–p'_2 diagram (Fig. 10a) and the position of the mean intercept value (Fig. 10b) closer to class 2 point than the plots of the Navia unit folds (Figs. 10c & d). The p'_1–p'_2 points from the Mondoñedo unit show lower dispersion than those of the Navia unit.

(3) *Folds in a multilayer*. Hand specimen-scale folds, folding a multilayer of Devonian marbles and metapelites (Fig. 11a) from the Axial Zone of the Pyrenees (N Spain), have been classified. In the p'_1–p'_2 diagram (Fig.

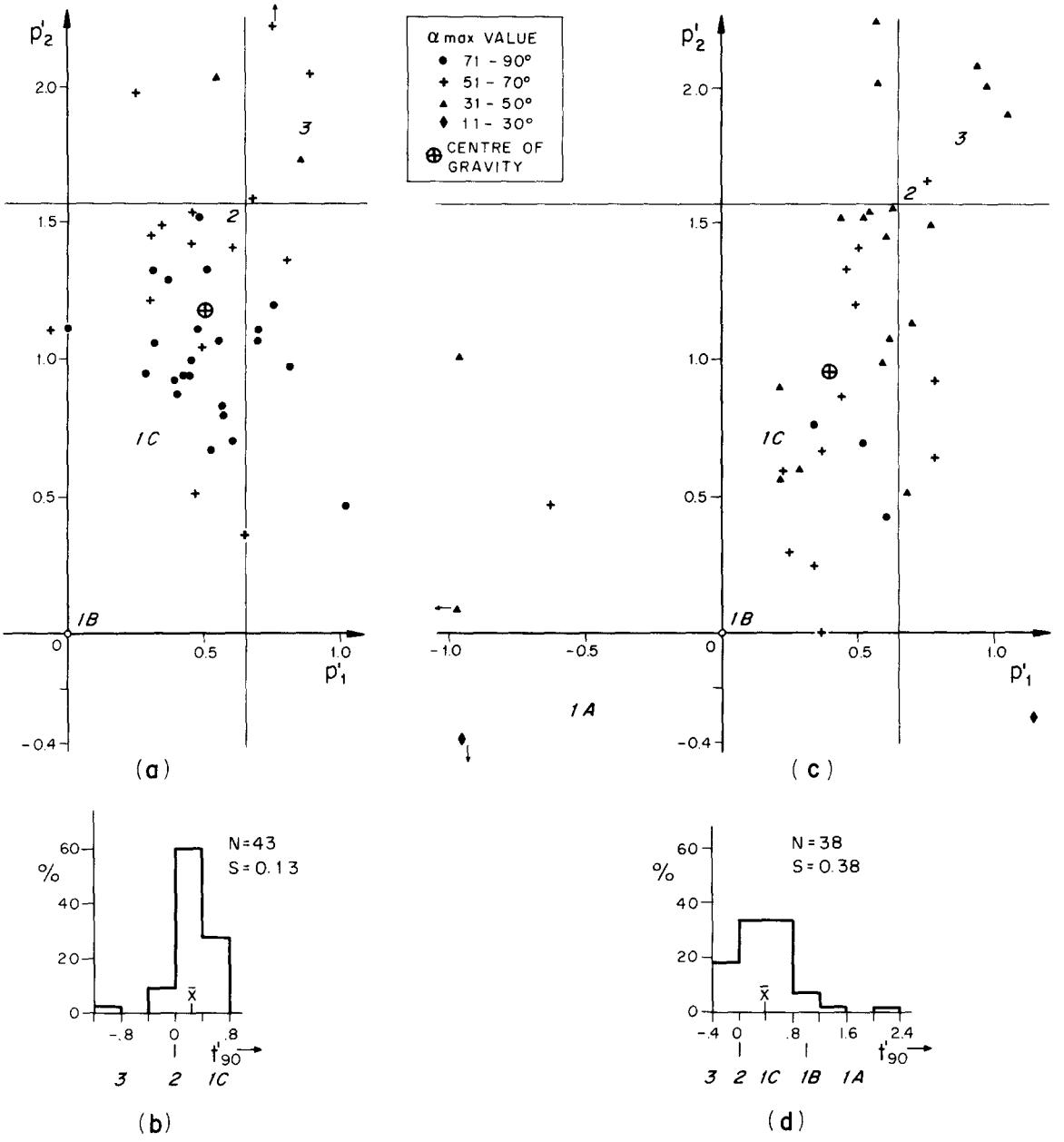

Fig. 10. p'_2–p'_2 diagram and intercept value histograms for F_1 folds deforming quartzite rocks in (a) & (b) the Mondoñedo Nappe unit and (c) & (d) the Navia unit (NW Spain).

11b), p'_1 values lower than 0.2 and p'_2 values lower than 0.6 are unusual. Most of these folds belong to classes 1C, 3 or to a combination of both. Folds in the multilayer show the mean intersection value (Fig. 11c) and the centre of gravity in p'_1–p'_2 diagram approaching class 2 folds. In the p'_1–p'_2 diagram, the points which represent folds in metapelitic layers have higher values of p'_1 and p'_2 than those in the marble layers. In Fig. 11(a), the folded layers have been differentiated according to the class they belong to. The fold geometry frequently varies from having limbs of class 1C to class 3–1C whereas limbs of class 3 alternate with limbs of class 1C–3.

Geometry of folded layers vs geometry of single folded surfaces

The fact that the geometry of a folded layer can be represented by its intercept value t'_{90} offers the possibility of relating such geometry to the shape of folded surfaces. According to Hudleston (1973a), the shape of a limb profile in a single folded surface can be represented by means of the ratio (b_3/b_1) between coefficients b_3 and b_1 of the Fourier series which is representative of this profile; this ratio can be obtained by the visual method devised by the quoted author. It is then possible to construct a diagram of b_3/b_1 against t'_{90} to relate the geometry of folded layers to the shape of folded surfaces. However, a problem arises because each folded layer is limited by two folded surfaces. One way of solving this problem is by representing the average value of b_3/b_1 for both surfaces. This type of diagram applied to folds in Fig. 11 shows that relationship between single folded layers shape and Ramsay's fold classes does not draw a trend (Fig. 12). Nevertheless, the graph shows the main features of the fold geometries.

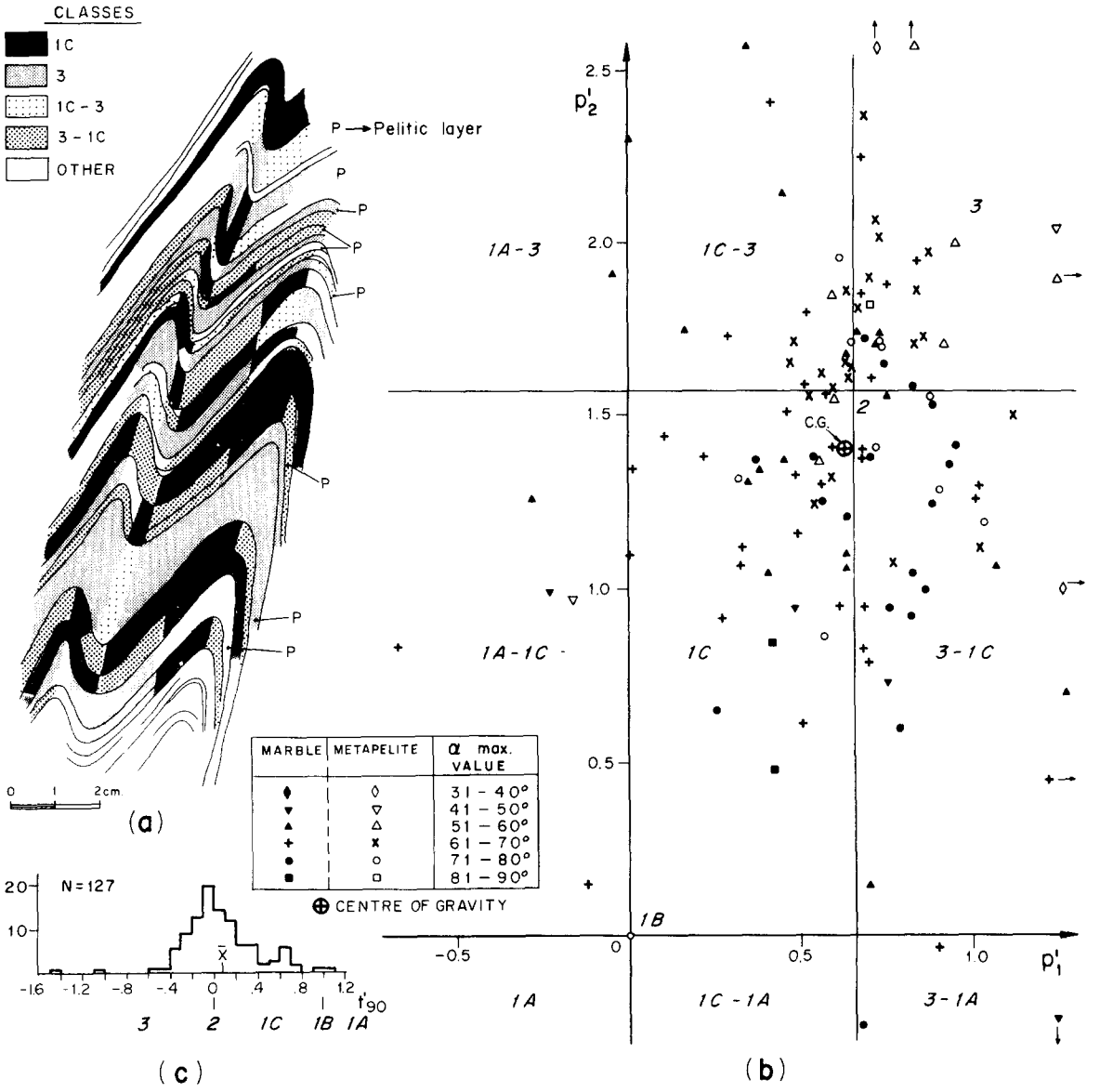

Fig. 11. (a) Small folds developed in a marble–metapelite multilayer in a Devonian rock sample (Benasque; Pyrenees; N Spain). (b) p'_1–p'_2 diagram. (c) Intercept values histogram.

DISCUSSION AND CONCLUSIONS

The p'_1–p'_2 diagram method presented in this paper offers several advantages. The method is easy and fast because it only involves the measurement of three values of the orthogonal thickness (t_0, $t_{\alpha_{max}}$ and $t_{\alpha_{max}/2}$) for each limb, that is represented by one point on the p'_1–p'_2 diagram. Therefore, the method allows representation of a large number of folds in a single diagram and also allows easy visualization of differences in geometry.

The parameters p'_1 and p'_2 reflect the geometry of t'_α curves, since they represent mean values of the curve slope for the corresponding sections. Thus, the points on the p'_1–p'_2 diagram are a good representation of the geometry of folded layers, allowing folds composed of two different classes to be distinguished and trends in changes in fold geometry to be noticed within a field of the diagram. In Ramsay's classification, the fold class is determined by the slope of the t'_α curves, rather than by their position within a given field of the α–t'_α diagram, and so a more accurate classification requires in addition the derivatives of t'_α. Another advantage of the p'_1–p'_2 method is that averaging the slope of the t'_α curve reduces the effect of the error in selecting reference points where the dip is taken as zero.

Once p'_1 and p'_2 are known, the intercept value t'_{90} is very easy to obtain, and represents a parameter that can be used as a one-dimensional statistical variable easy to analyse. The use of this value alone implies a loss of information on the geometry of individual folds, because folds with different t'_α curves may have the same t'_{90} value. However, it constitutes a useful complement of the p'_1–p'_2 method.

The intercept value t'_{90} can be related with other geometrical fold parameters. In this way, the b_3/b_1 vs t'_{90} graph allows both the geometry of single folded surfaces and the geometry of folded layers to be shown.

The proposed fold classification method discriminates the different geometries of folds throughout a multilayer and allows a comparative analysis of folds in regional studies. This classification method also permits the comparison of natural fold geometry and the geometry of

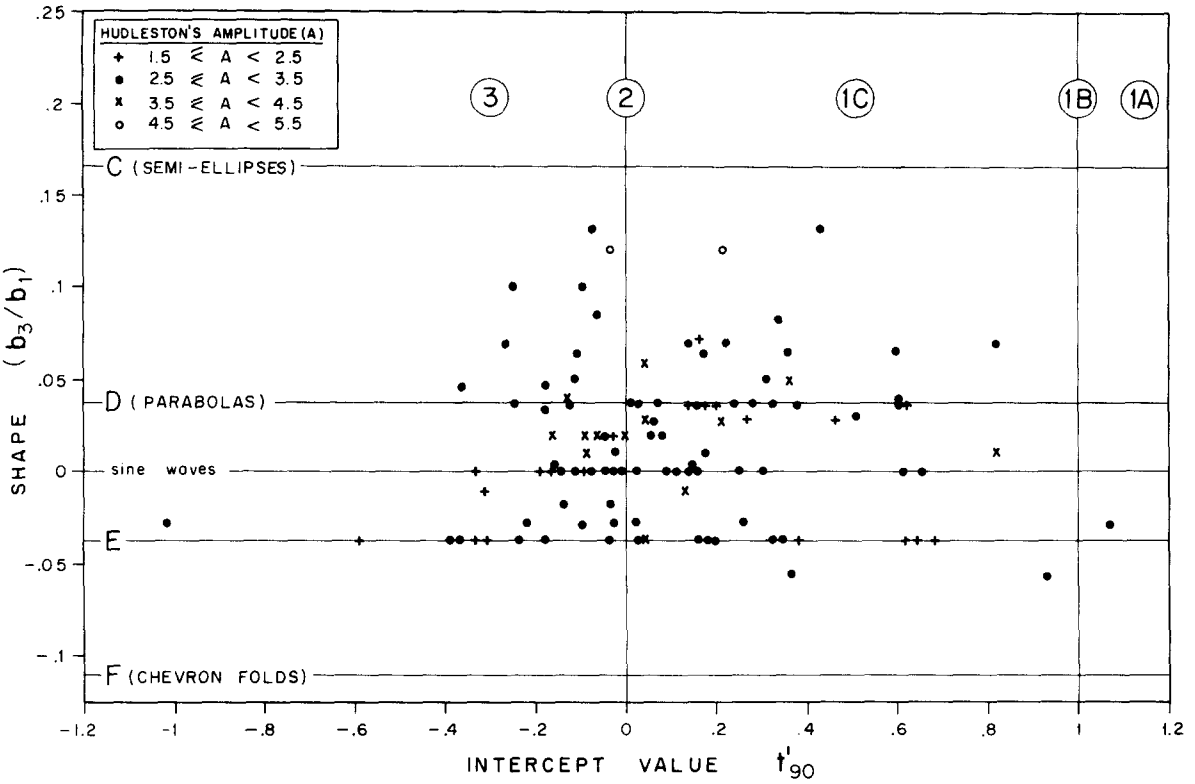

Fig. 12. Diagram showing the intercept value (t'_{90}) against the single folded surface shape (b_3/b_1) for folds in Fig. 11. C, D, E and F are the shapes in Hudleston's classification. 1A, 1B, 1C, 2 and 3 are the fold classes in Ramsay's classification. The points on the graph show a stratified pattern due to the non-continuous range of b_3/b_1 value in Hudleston's (1973a) visual classification method.

folds obtained from laboratory or deduced from theoretical studies, in order to provide a better understanding of the folding process.

Acknowledgements—This work received financial support from Project C.I.C.Y.T. GEO-89 372-CO2-01. I wish to thank the Structural Geology group of Oviedo University for many helpful discussions. I also thank D. L. Brown, A. González Pozueta, A. Ojanguren and S. Phipps for comments and help with the English version of the manuscript. I should also like to extend my thanks to N. Mancktelow, an anonymous referee, and S. H. Treagus, whose comments and suggestions helped to clarify and improve the manuscript.

REFERENCES

Bastida, F. 1980. Las estructuras de la primera fase de deformación herciniana en la Zona Asturoccidental-leonesa (costa cantábrica, NW de España). Unpublished thesis, University of Oviedo.

Davis, G. H. 1975. Gravity-induced folding off a gneiss dome complex, Rincon Mountains, Arizona. *Bull. geol. Soc. Am.* **86**, 979–990.

Hudleston, P. J. 1973a. Fold morphology and some geometrical implications of fold development. *Tectonophysics* **16**, 1–46.

Hudleston, P. J. 1973b. The analysis and interpretation of minor folds developed in the Moine rocks of Monar, Scotland. *Tectonophysics* **17**, 89–132.

Ramsay, J. G. 1962. The geometry and mechanics of formation of "similar" type folds. *J. Geol.* **70**, 309–327.

Ramsay, J, G. 1967. *Folding and Fracturing of Rocks*. McGraw-Hill, New York.

Ramsay, J. G. & Huber, M. 1987. *The Techniques of Modern Structural Geology, Volume* 2: *Folds and Fractures*. Academic Press, London.

Treagus, S. H. 1982. A new isogon-cleavage classification and its application to natural folds and model fold studies. *Geol. J.* **17**, 49–64.

Twiss, R. J. 1988. Description and classification of folds in single surfaces. *J. Struct. Geol.* **10**, 607–623.